

DETECTORS FOR IMAGING IN RADIATION THERAPY

I. G. Valais¹, P. C. Xydias²

¹Department of Medical Instruments Technology, Technological Educational Institution of Athens, Ag. Spyridonos, Aigaleo, 122 10 Athens, Greece, e-mail: ivalais@teiath.gr

²Radiation Therapy Department, Iatropolis S.A., 56 Ethnikis Antistaseos str., 15231 Athens, Greece

Abstract. *Despite the many advances in patient positioning, dose deliverance as intended remains a difficult practical issue due to a number of complicating factors. Various techniques and methods have been developed over the years for accurate patient positioning. It has long been recognized that the use of the therapy x-ray beam itself to create portal images can be of significant benefit in assuring correct delivery of the radiation dose. The present study is a brief overview of the detectors incorporated on electronic portal imaging devices imposed by the nature of the application and the physics of the imaging source. It is a summary of the challenges and constraints inherent to portal imaging along with a concise, historical review of the technologies that have been explored and developed. This is followed by a detailed description of a new, high performance, portal imaging technology, which is presently undergoing commercial introduction.*

1 INTRODUCTION

Radiation therapy treatment is designed to treat the defined tumor and spare the surrounding normal tissue from receiving doses above specified dose tolerances. There are many factors that may contribute to differences between the planned dose distribution and the delivered dose distribution. One such factor is uncertainty in patient position on the treatment unit. Planning Target Volume (PTV) margins are the most widely used method to correct geometric uncertainties. They were used to compensate for localization errors during treatment. This resulted in healthy human tissues receiving unnecessary doses of radiation during treatment. The need for decreasing the dose to surrounding healthy tissues, can be accomplished by improving precision and accuracy, allowing for increased radiation to the tumor for control [1].

One of the most widely used radiation oncology technologies on the market today is image guided radiation therapy (IGRT). IGRT allows images to be acquired immediately before a patient receives treatment to confirm that the beam is going to hit the intended target. The variety of image gathering hardware used in planning includes Computed Tomography (CT), Magnetic Resonance Imaging (MRI), and Positron Emission Tomography (PET) among others. It enables radiation treatment to be delivered more accurately and at higher doses to eradicate the tumor. However, there is clearly a connection between the imaging processes as IGRT relies directly on the imaging modalities from planning as the reference coordinates for localizing the patient [1, 2].

Currently, certain radiation therapy techniques employ the process of Intensity Modulation Radiotherapy (IMRT). This form of radiation treatment uses computers and linear accelerators to create a three-dimensional radiation dose map, specific to the target's location, shape and motion characteristics. Because of the level of precision

required for IMRT, detailed data must be gathered about tumor locations.

Despite these and many other advances in patient positioning, dose deliverance as intended remains a difficult practical issue due to a number of complicating factors. For example, the size and shape of the tumor can change during the course of treatment, which typically extends over a number of weeks. In addition, the position of the tumor in the patient may vary from treatment to treatment, or even during treatment, due to such influences as breathing, the degree of extension of the bladder and changes in patient positioning. Moreover, errors in the set-up of the patient and/or of the beam collimators are also possible. For these reasons, it has long been recognized that the use of the therapy x-ray beam itself to create portal images can be of significant benefit in assuring correct delivery of the radiation dose [3, 4].

Munro (1999) [4], presents a highly detailed review of the history and technology of electronic and non-electronic portal imagers along with a discussion of a variety of theoretical and practical considerations and issues. He also summarized features of the two Electronic Portal Imaging Device (EPID) technologies commercially available at the time.

The present study is a brief overview of the detectors incorporated on electronic portal imaging devices imposed by the nature of the application and the physics of the imaging source. This is followed by a detailed description of a new, high performance, portal imaging technology, which is presently undergoing commercial introduction and which emerged from research initiated in the late 1980s.

2 OVERVIEW OF PORTAL IMAGING DEVICES

2.1 Camera–Mirror–Lens-based EPID systems

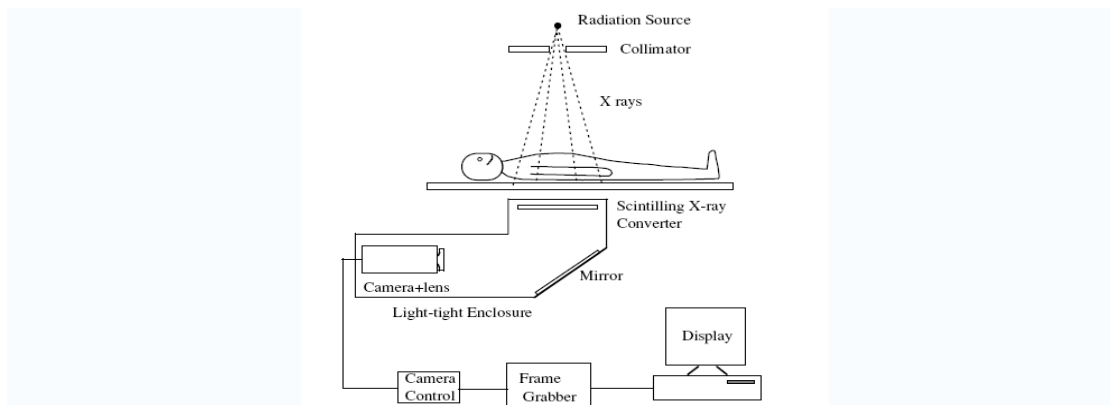


Figure 1. Schematic illustration of a camera-based EPID with the x-ray detector (a phosphor screen) optically coupled to the camera using a mirror and lens.

In the camera-mirror-lens-based EPID system, the converter consists of a flat metal plate (typically an ~1 to 1.5 mm copper, steel or brass plate) and a gadolinium oxysulfide ($Gd_2O_2S:Tb$) phosphor screen. The metal plate serves to convert incident primary x-rays into high energy electrons, some of which escape the plate into the phosphor, as well as to block low-energy, scattered radiation which would otherwise reduce the contrast of the imaging system. The camera and lens serve to capture a

fraction of this emerging light and transform it into a video signal that is then sent to other hardware for digitization, processing, display and archiving. The optical components are enclosed in a light-tight housing to exclude light signal from sources other than the phosphor. The mirror set at a 45° angle serves to direct the light out of the radiation field towards the camera to avoid degradation of camera electronics from direct radiation exposure. Depending on the thickness of the phosphor and the energy of the radiotherapy beam, on the order of only ~2–4% of the incident x-rays interact and generate measurable signal in such systems [5].

One of the major advantage of this system is that the converter can cover all (or at least a very large fraction) of the portal field and the camera can sense the light signal from the entire converter simultaneously. Consequently, all of the radiation passing through the patient and incident upon the converter has the potential of generating signal in the camera and clinically useful images can be produced with as few as a couple of monitor units.

One disadvantage of this approach is that the optical components and their light-tight housing are relatively bulky and present an encumbrance in the vicinity of where the therapists set up the patient. Additionally, the optics of the system only allow those light photons emerging from the phosphor within a small cone subtended by the lens of the camera to generate signal in the camera [6]. As a result, only 0.1–0.01% of the light emerging from the phosphor reaches the sensor of the camera [6]—an effect which reduces image quality.

2.2 Scanning matrix ionization chamber EPID systems

Like the camera–mirror–lens-based systems described above, the EPID system based on a scanning matrix ionization chamber uses of a liquid ionization chamber formed by two planes of electrodes separated by a 0.8 mm gap (Figure 2). The gap is filled with a fluid (2,2,4-trimethylpentane) which acts as an ionization medium when the chamber is irradiated. Each electrode plane consists of 256 parallel wires spaced 1.27 mm apart. The electrodes on the two planes are oriented perpendicularly to each other thereby forming a matrix of 256×256 ionization cells that provide a detection area of $32.5 \times 32.5 \text{ cm}^2$. A 1 mm thick plastoferrite plate positioned over the ionization chamber serves the same purpose as the metal plate in camera-based systems.

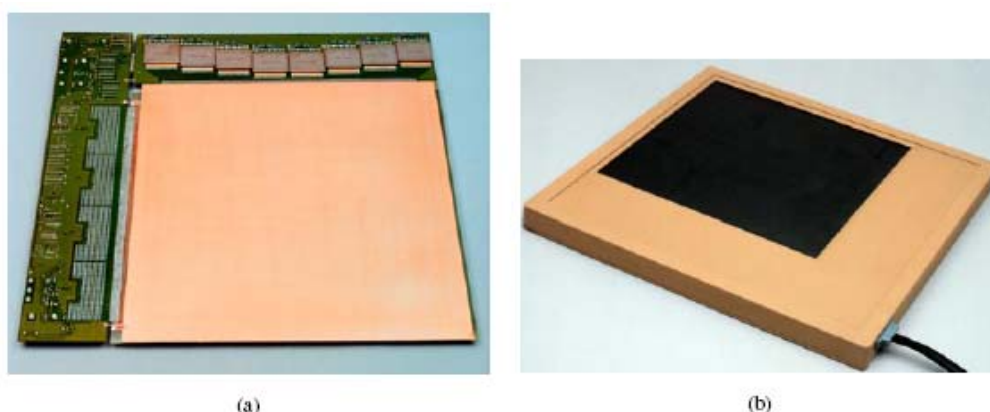


Figure 2. Photos of the matrix ionization chamber EPID design. (a) View of interior components. (b) Early packaging of system in a film-cassette-like housing, taken from [6]

The ionization medium also serves to convert primary x-rays into high-energy electrons and, analogous to the phosphor screen in some camera-based systems, transforms a fraction of the energy of the high-energy electrons passing through it into a measurable (ion) signal. A high-voltage supply is used to apply a 300 V bias to each electrode individually on one of the planes (the high voltage plane). The electrodes on the other plane (the signal plane) are individually connected to electrometers. The entire imager consists of the matrix ionization chamber, a 256-channel high-voltage switching system, a 256-channel electrometer, and control electronics. Full resolution readout of the imager is achieved by applying the high voltage to each of the electrodes on the high voltage plane in succession (for about 20 ms) and recording the signal generated in each of the 256 [5].

Important advantages of this system include the compactness of the detector, approaching that of a film cassette, and the lack of geometric distortions in the image. The most significant disadvantage of this approach is that the utilization of incident x-ray quanta is inferior to that of a true area detector since, for full-resolution readout, only a single electrode on the high voltage plane is switched on at a time [5].

2.3 Active matrix, flat-panel imager (AMFPI) EPIDs

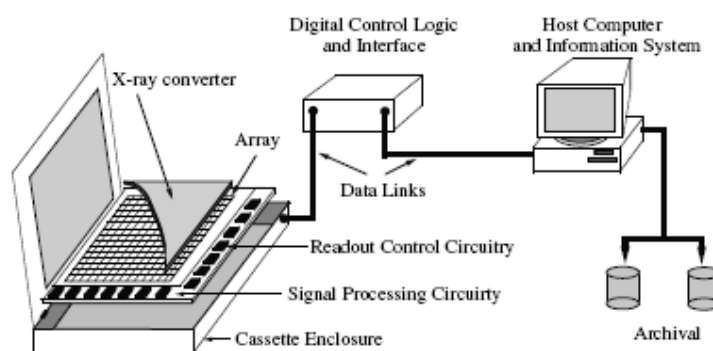


Figure 3. Schematic illustration of the elements of an active matrix, flat-panel imager (AMFPI), taken from [7].

AMFPI technology features the array which consists of an ~1mm thick glass substrate on which thin-film electronic circuits reside. These circuits (Figure 3) are created through a series of semiconductor processing steps involving plasma enhanced, chemical vapor deposition (PECVD), etching and passivation—typically involving 5–10 sets of photolithographic masks [7]. Each pixel in an active matrix array incorporates a thin-film switch connected to some form of capacitive element. The pixels are organized in a two-dimensional grid and the conductivity of the pixel switches is controlled through variation of the voltage of control lines with each control line connected to all of the pixel switches in a single row. (The control lines are often called gate control lines for array designs incorporating a pixel switch consisting of a thin-film transistor).

The pixel switches are generally kept non-conducting so that charge generated directly or indirectly by incident radiation interacting in an overlying x-ray converting material is integrated in the capacitive element of each pixel. Readout of these imaging signals from the capacitive elements is accomplished by rendering the pixel switches conducting. Typically, one row of pixels is read out at a time for maximum

spatial resolution, although multiple rows can be read out at a time for faster readout at lower resolution. When the pixel switches along a given row are made to conduct, imaging signals stored in the pixels are sampled by external peripheral electronics by means of data lines, with each data line connected to all the pixel switches in a given column. This action also reinitializes the pixels—although additional initialization steps may be required depending on the type of switch and the nature of the converter.

The general organization of these imaging arrays is parallel to that of active matrix liquid-crystal displays (AMLCDs, commonly used for laptop computers).

3 AMFPI DESIGNS FOR PORTAL IMAGING

The pixel switches employed for the majority of AMFPI designs are thin film transistors (TFTs) fabricated from hydrogenated amorphous silicon (a-Si:H) (Figure 4). Two general approaches can be distinguished based on how this imaging signal is generated and stored in the pixels [7]:

- (a) Indirect detection AMFPIs use an x-ray converter consisting of a combination of a metal plate and a scintillator—with the scintillator positioned directly over the photosensor integrated into the array. Light entering the photosensor is converted into electron–hole pairs, one electron–hole pair per detected light photon. The structure of the photosensor also forms the capacitive element in each pixel where this signal is stored until readout.
- (b) Direct detection AMFPIs use an x-ray converter consisting of a combination of a metal plate and a photoconductor—with the photoconductor electrically coupled to a separate capacitor built into each pixel. The radiation generates electron–hole pairs in the photoconductor and this imaging signal is stored in the pixel capacitors until readout.

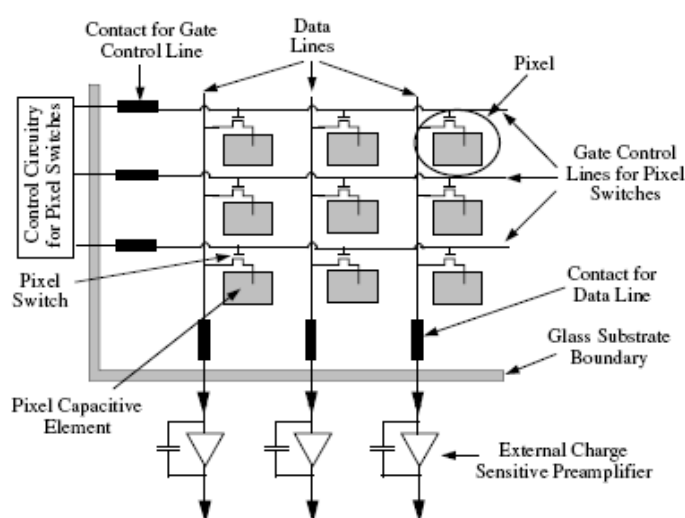


Figure 4. Schematic illustration of a corner of an indirect or direct detection active matrix, flat panel imaging array illustrating the matrix addressing scheme of such designs. Also illustrated is external peripheral control circuitry that is connected to the array via peripheral contacts—one contact for each gate control line and each data line. This circuitry controls the conductivity of the pixel switches and amplifies the pixel signals. As an example, the pixel switches are represented as TFTs but diode-based

switches are also used in some diagnostic imager designs. The capacitive element depicted for each pixel in the figure corresponds to a photosensor for an indirect detection array and a storage capacitor for a direct detection array, taken from [7]

3.1 Indirect detection AMFPIs EPIDs

The photosensor is a continuous a-Si:H photodiode to increase the optical fill factor the fraction of the pixel that is sensitive to light from the scintillator [8]. The scintillator incorporated in present systems is columnar CsI(Tl) (Figure 5). Indirect detection AMFPIs offer a variety of advantages for the portal imaging application [3].

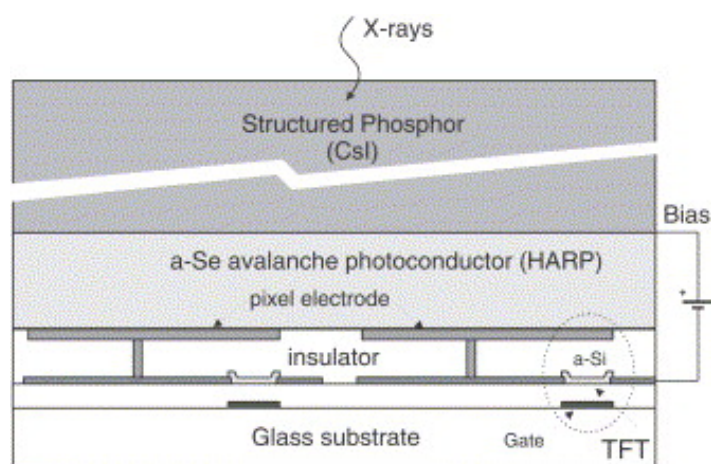


Figure 5. Schematic diagram showing the concept of indirect AMFPI with TFT readout method, using a columnar CsI(Tl) scintillator.

- (a) This solid state technology facilitates the creation of compact detectors offering real-time, digital readout.
- (b) Allows the creation of very large-area arrays, monolithic active matrix flat-panel arrays as large as 41×41 cm² have been produced. If required by the application, even larger detectors should be possible [9].
- (c) The arrays and their acquisition systems may be designed to provide both radiographic readout (i.e. capture of single frames) or fluoroscopic readout (e.g. up to 30 frames per second [10]).
- (d) The signal response of the pixels is highly linear (Antonuk et al 1998) and the technology can be configured for dosimetric measurements [11].
- (e) The a-Si:H TFTs and photodiodes are highly resistant to radiation damage [12]—even at the very high doses to which a portal imager could be exposed (in excess of 10^4 Gy per year).
- (f) High degree of image quality. AMFPI-based EPIDs are capable of using on the order of 50% of the light emitted from the scintillator. This value is several orders of magnitude larger than optical transfer efficiencies for camera-mirror-lens-based systems. Consequently, secondary quantum sinks in the number of detected optical quanta, which limit the performance of camera-based EPIDs, are absent in AMFPI-based EPIDs allowing this technology to offer x-ray quantum limited imaging [11].

3.2 Direct detection AMFPIs EPIDs

In the direct detection approach, a continuous layer of photoconductive material is deposited over the surface of the array [13]. Each pixel has an auxiliary storage capacitor connected to the pixel switch as well as to a collection electrode that serves to gather signal from the photoconductor (Figure 6). The photoconductor currently used in commercial AMFPIs for diagnostic imaging is amorphous selenium (a-Se) with thicknesses up to $\sim 1000 \mu\text{m}$ (Choquette et al 2000). (Other materials such as lead iodide (PbI_2), mercuric iodide (HgI_2), and cadmium telluride (CdTe) are also under examination for diagnostic imaging [14] Given that $1000 \mu\text{m}$ of a-Se would have an estimated x-ray quantum detection efficiency of $\sim 3\%$ for a 6 MV beam, the use of this material in a direct detection AMFPI for portal imaging would be of interest.

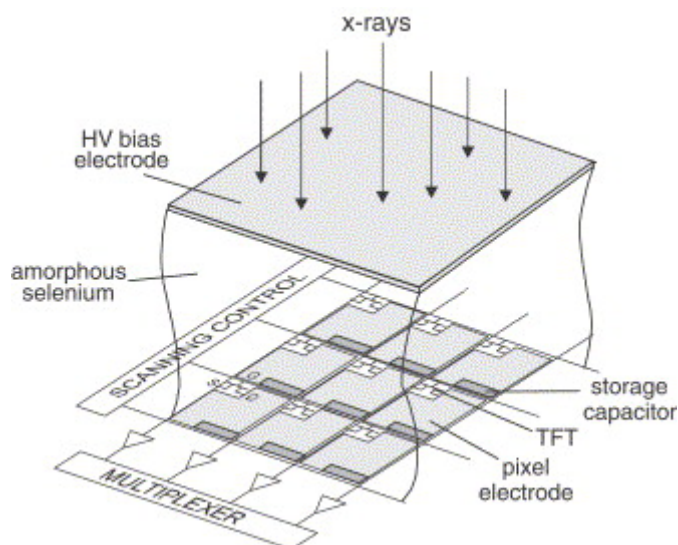


Figure 6. Schematic diagram showing the concept of direct AMFPI using TFT readout method.

3 IMPROVING EPID PERFORMANCE

One approach towards increasing the x-ray quantum detection efficiency for portal imaging involves the use of the kinestatic charge detection (KCD) technique originally developed for diagnostic imagers [15]. The KCD approach, illustrated in Figure 7, involves the use of an x-ray detector that is scanned across the field of view. The detector consists of an x-ray detection volume and a signal collection volume. In the design, while the detection volume is continuous, the signal collection volume consists of a linear array of n discrete charge detection elements. Incident x-rays interact and generate charge in the detection volume.

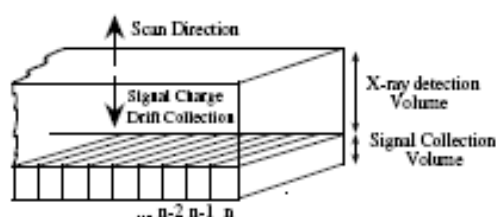


Figure 7. Schematic diagrams illustrating the kinestatic charge detection (KCD) technique. Diagram of an n -channel KCD illustrating the x-ray detection and signal collection volumes and the anti-parallel scan and signal charge drift directions.

An electric field applied across this volume drives a portion of this charge toward the signal collection elements that serve to continuously produce a spatially discrete set of n signals that may be amplified and digitized. Central to the KCD technique is the fact that the detector is mechanically scanned at a speed equal and opposite to the signal charge drift velocity, in a direction perpendicular to that of the x-ray beam. This procedure makes the secondary ionization cloud created by the interacting x-rays stationary relative to the coordinate system of the radiation source. Thus, for a given incident x-ray trajectory, charge is integrated along a single line in the volume of the detector that is sampled all together by a signal collection element. The signal from each collection element is integrated over an appropriate time interval, m times per scan, so as to produce an $n \times m$ array of numbers which constitutes a two-dimensional image. Early theoretical and empirical studies [15] predict high x-ray quantum detection efficiency ($\sim 36\%$) and forecast that the system would offer high spatial resolution, high contrast resolution, and negligible scatter acceptance.

A novel gas detector concept [16], incorporates the use of a gas electron multiplier (GEM)—an amplification structure recently developed by Sauli at CERN [17] (Figure 8). The GEM is a simple device that provides efficient multiplication of electrons in a gas detector with a gain on the order of 10^3 – 10^4 . One possible configuration for the imager consists of a single chamber filled with gas at atmospheric pressure with two parts: an upper part to image diagnostic-energy x-rays and a lower part to image megavoltage-energy x-rays. In this realization, diagnostic x-rays interact in a gas converter followed by a GEM. In the lower part of the detector, several converter plates, followed by GEMs, are incorporated in the design to increase the detection efficiency of the megavoltage x-rays.

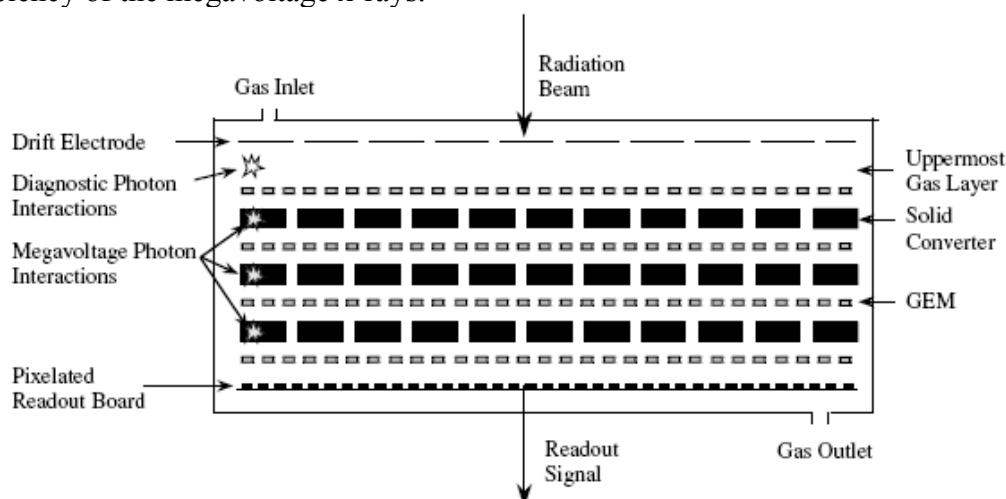


Figure 8. Schematic drawing of a possible configuration, of a dual-energy device for diagnostic and portal imaging under development. This configuration incorporates an upper detector for diagnostic imaging and a lower portion, consisting of three sets of solid converters and GEMs (gas electron multipliers) for portal imaging.

An electric field is applied across the chamber to allow signal electrons generated by the interacting x-rays to drift down to an electronic readout plate offering $1 \times 1 \text{ mm}^2$ pixelated readout. Holes in the converter plates allow signal generated above the plates to pass through to the readout plate. It is estimated that the device will offer a $40 \times 40 \text{ cm}^2$ detection area and will allow very fast readout after every radiation pulse.

Another approach is using a polymer microfabrication for thick, high aspect-ratio segmented x-ray conversion screens based on UV lithography [18]. The x-ray conversion screens were fabricated on 4 inch glass substrates with an SU-8 thickness of up to $\sim 2.5 \text{ mm}$. After metallization, the SU-8 cells are filled with a scintillating phosphor. Typically, this is a powder consisting of a material such as terbium-doped gadolinium oxysulfide, $\text{Gd}_2\text{O}_2\text{S:Tb}$ (GOS), which emits visible light upon excitation by the x-rays. GOS emits in the green wavelength range, which is where the amorphous silicon p-i-n photodiodes of the image sensor array have their highest sensitivity.

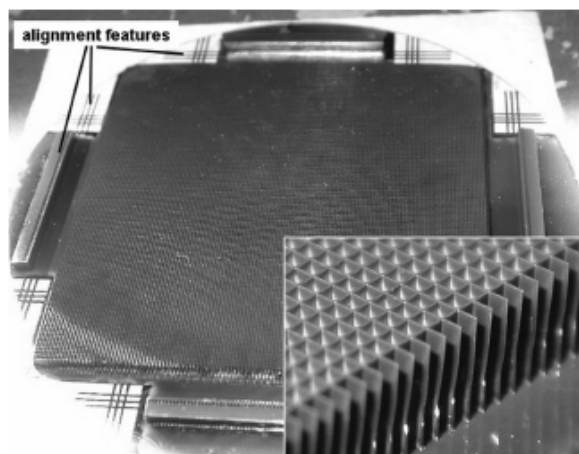


Figure 9. Photograph of 2.5 mm high SU-8 cell structures ($508 \mu\text{m}$ pitch) on a 4 inch diameter glass wafer. The SU-8 cells are sputter-coated with aluminum. Alignment features on the periphery assist in the alignment of the conversion screen to the image sensor array. The inset shows a close-up view of the cells, taken from [18].

As illustrated Figure 9, the phosphor screen is laid directly onto the image sensor. The cells of the conversion screen must be aligned to the pixels of the image sensor array. The surface of the phosphor screen has to be smooth and flat to guarantee close contact between the screen and the surface of the image sensor array, otherwise light can leak between neighboring cells.

Recently proposed by El-Mohri *et al* (2009) [19], an active pixel imager incorporating pixel-level amplifiers based on polycrystalline-silicon thin-film transistors (PSI-TFT), using $\text{Gd}_2\text{O}_2\text{S:Tb}$ scintillating screens. The prototypes, employ various pixel circuits and incorporate a continuous photodiode structure. They also incorporate an amplification circuit in each pixel refer to as an “active pixel” (AP) architecture (Figure 10).

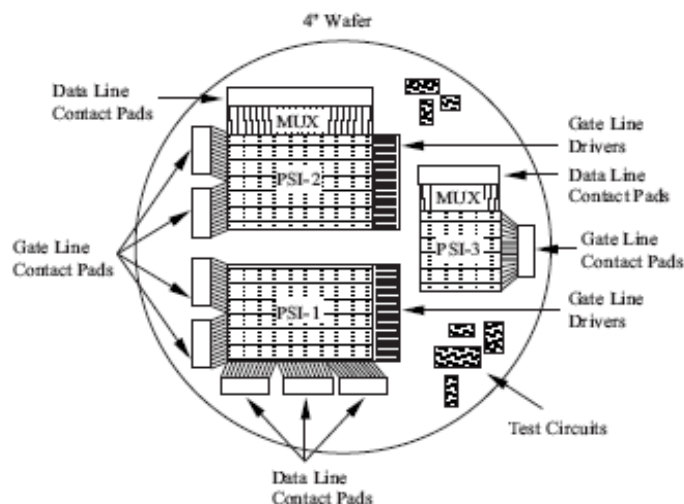


Figure 10. Schematic diagram illustrating the general features and layout of the three poly-Si array designs, PSI-1, PSI-2, and PSI-3, on a 4 inch wafer. The contact pads located at the periphery of the arrays were used to connect the data and gate lines to external preamplifier and gate driver circuits. For PSI-2 and PSI-3, these contact pads connect to the array data lines via poly-Si multiplexer circuitry (labeled MUX), which reduces the number of contacts by factors of 16 and 8, respectively, taken from [19].

Unlike conventional designs, the TFT employs a dual gate structure in order to reduce the elevated levels of leakage current that result from the higher mobilities offered by poly-Si material. These arrays [19] have a pixel format of $\sim 384 \times 256$ pixels and a pitch of $90 \mu\text{m}$, giving an active area of $\sim 3.45 \times 2.30 \text{ cm}^2$. PSI-1 (which has been previously characterized) provides a reference for the performance of an array based on poly-Si TFTs, without in-pixel amplification. These prototypes provided an initial, empirical demonstration that a specified level of additional system gain can be achieved through the implementation of active pixel architectures based on poly-Si TFTs. In addition, the incorporation of a novel continuous photodiode structure, located largely above the plane of the pixel TFTs (thereby maximizing the area available for other pixel circuit elements), has been shown to further increase system gain by providing optical fill factors that are close to unity.

Ultimately, the achievement of optimized signal-to-noise behavior in future prototypes will require improved design and fabrication of the arrays, as well as a detailed understanding and quantification of all noise sources. The latter can be achieved through a combination of circuit simulations and analytical noise calculations, employing empirical data obtained from individual poly-Si TFTs [19].

REFERENCES

- [1] Jaffray, DA, Bissonnette JP, Craig T. (1999). "X-ray Imaging for Verification and Localization in Radiation Therapy in Modern Technology of Radiation Oncology (suppl. 1)". *Modern Technology of Radiation Oncology*. Madison, WI: Medical Physics Pub. [ISBN 0-944838-38-3](#).
- [2] Dawson, LA, Sharpe, MB (2006), "Image-guided radiotherapy: rationale, benefits, and limitations", *Lancet Oncol.* **7** (10), pp. 848-858

- [3] Antonuk, L.E (2002). “Electronic portal imaging devices: a review and historical perspective of contemporary technologies and research”, *Phys. Med. Biol.* **47**, R31-65.
- [4] Munro P, Rawlinson J A and Fenster A (1988). “Therapy imaging: source sizes of radiotherapy beams”, *Med. Phys.* **15**, pp.517–24
- [5] Herman M G, Balter J M, Jaffray D A, McGee K P, Munro P, Shalev S, Van Herk M and Wong J W (2001). “Clinical use of electronic portal imaging: report of AAPM radiation therapy committee task group 58”, *Med. Phys.* **28**, pp. 712–37
- [6] Munro P (1995). “Portal imaging technology: past, present, and future”, *Semin. Radiat. Oncol.* **5**, pp. 115–33
- [7] Antonuk L E, El-Mohri Y, Huang W, Jee K-W, Siewerdsen J H, Maolinbay M, Scarpine VE, Sandler H and Yorkston J (1998). “Initial performance evaluation of an indirect-detection, active matrix flat-panel imager (AMFPI) prototype for megavoltage imaging”, *Int. J. Radiat. Oncol. Biol. Phys.* **42**, pp. 437–54
- [8] Mulato M, Ready S, Van Schuylenbergh K, Lu J P and Street R A (2001) “Cross-talk and lateral conduction effects in continuous-sensor amorphous silicon imagers”, *J. Appl. Phys.* **89** pp. 8193–201.
- [9] Colbeth R E, Allen M J, Day D J, Gilblom D L, Klausmeier-Brown M E, Pavkovich J, Seppi E J and Shapiro E G (1997). “Characterization of an amorphous silicon fluoroscopic imager” *Proc. SPIE* **3032**, pp. 42–51
- [10] Antonuk L E, Yorkston J, Huang W, Siewerdsen J and Street R A (1993). “Considerations for high frame rate operation of two-dimensional a-Si:H imaging arrays”, *Mater. Res. Soc. Symp. Proc.* **297**, pp. 945–50.
- [11] El-Mohri Y, Jee K-W, Antonuk L E, Maolinbay Mand Zhao (2001). “Determination of the detective quantum efficiency of a prototype megavoltage indirect detection, active matrix flat-panel imager”, *Med. Phys.* **28**, pp. 2538–50
- [12] Antonuk L E, Yorkston J, Huang W, Sandler H, Siewerdsen J H and El-Mohri Y (1996). “Megavoltage imaging with a large area, flat-panel, amorphous silicon imager”, *Int. J. Radiat. Oncol. Biol. Phys.* **36** pp 661–72
- [13] Zhao W and Rowlands J A (1995) “X-ray imaging using amorphous selenium: feasibility of a flat-panel self-scanned detector for digital radiology” *Med. Phys.* **22**, pp. 1595-1604.
- [14] Street R A, Mulato M, Schieber M, Hermon H, Shah K, Bennett P, Dmitryev Y, Ho J, Lau R, Meerson E, Ready S E, Reisman B, Sado Y, VanSchuylenbergh K, Vilensky A and Zuck A (2001). “Comparative study of PbI₂ and HgI₂ as direct detector materials for high resolution x-ray image sensors” *Proc. SPIE* **4320** pp. 1–12
- [15] DiBianca F, Samant S, Laughter J, Rasmussen J and Rodriguez C (1997). “Use of a kinesthetic charge detector for megavoltage portal imaging”, *Proc. SPIE* **3032** pp. 195–201
- [16] Iacobaeus C, Brahme A, Danielsson M, Fonte P, Ostling J, Peskov V and Wallmark M (2001). “A novel portal imaging device for advanced radiation therapy”, *IEEE Trans. Nucl. Sci.* **48** pp. 1496–502
- [17] Sauli F (1997). “GEM: a new concept for electron amplification in gas detectors”, *Nucl. Instrum. Methods A* **386** pp. 531–4
- [18] Daniel J.H., Sawant A., Teepe M., Shih C., Street R.A., and Antonuk L.E., (2007). “Fabrication of high aspect-ratio polymer microstructures for large-area electronic portal x-ray imagers”, *Sens Actuators A Phys.* **140**(2) pp. 185–193.

- [19] El-Mohri Y, Antonuk LE., Koniczek M, Zhao Q, Li Y, Street RA. and Lu JP, (2009). “Active pixel imagers incorporating pixel-level amplifiers based on polycrystalline-silicon thin-film transistors” *Med. Phys.* **36** (7) pp. 3340-3355.